

This is a repository copy of *Bio-inspired Anomaly Detection for Low-cost Gas Sensors*.

White Rose Research Online URL for this paper:
<https://eprints.whiterose.ac.uk/182885/>

Version: Accepted Version

Proceedings Paper:

Liu, Junxiu, Harkin, Jim, McDaid, Liam et al. (8 more authors) (2019) Bio-inspired Anomaly Detection for Low-cost Gas Sensors. In: 18th International Conference on Nanotechnology, NANO 2018. 18th International Conference on Nanotechnology, NANO 2018, 23-26 Jul 2018 Proceedings of the IEEE Conference on Nanotechnology . IEEE Computer Society , IRL .

<https://doi.org/10.1109/NANO.2018.8626301>

Reuse

["licenses_typename_other" not defined]

Takedown

If you consider content in White Rose Research Online to be in breach of UK law, please notify us by emailing eprints@whiterose.ac.uk including the URL of the record and the reason for the withdrawal request.

Bio-inspired Anomaly Detection for Gas Sensors

Junxiu Liu¹, Jim Harkin¹, Liam McDaid¹, Shvan Karim¹, Alan G. Millard², James Hilder², Simon Hickinbotham², Anju P. Johnson², Jon Timmis², David M. Halliday², Andy M. Tyrrell²

¹ School of Computing, Engineering and Intelligent Systems, Ulster University, Derry, UK, BT48 7JL

² Department of Electronic Engineering, University of York, York, UK, YO10 5DD

Abstract—This paper proposes a novel anomaly detection method for gas sensors using spiking neural network principles. The synapse models with excitatory/inhibitory responses and a single spiking neuron are employed to develop the bio-inspired anomaly detector for a single gas sensor. The approach can detect anomalies in the data, which is collected by the gas sensor by identifying rapid changes rather than a magnitude threshold. In particular, the false-positive detections due to drifts of low-cost sensors are minimised using the proposed bio-inspired approach. Using the chemicals of surgical spirits and isobutanol as test substances, experiments were carried out to evaluate the proposed method. Results demonstrate that gas anomalies can be detected when the chemical substances are presented to the sensor. In addition, results show that the approach can detect under the presence of sensor drift. The proposed bio-inspired detector was implemented on FPGA hardware, which demonstrates relatively low resources. Compact and energy efficient CMOS-based implementations of the synapse are also available which supports the low-cost potential applications of this approach, e.g. use in safety with drones and ground robots in hazardous scene detection.

I. INTRODUCTION

In security and safety applications the non-invasive detections of unusual substances are critical, such as baggage screening, illegal liquid detection, air quality analysis etc. A common non-invasive pathway for detection is via sensing the air. Such systems should have the capabilities to deal with different conditions including: a) distinguishing the normal (background) and abnormal (anomaly) substances which are released into the air, and b) making detection decisions taking account of the natural daily variations, and also the variations caused by the environments and the monitoring systems themselves. The drift caused by the environment, or the aging of the electronic components, is more prominent in lower cost sensors. Therefore, detector systems should be able to sense the anomalies while under the presence of such sensor drift. Anomalies occur over time where concentration of the gas are sensed by a sensor. Spiking neural networks (SNNs) are temporal based and use synapses and neurons to detect patterns/changes over time. SNNs demonstrated the capability in detecting abnormal conditions such as errors and also demonstrated a compact area/power requirements [1]. Therefore in this paper, inspired by the temporal behaviours of synapses and spiking neurons, we explore their application for the anomaly detection of gases, where sensors produce dynamic/pulsing outputs when a gas is sensed. This task is compounded with the challenges of taking into account hardware sensor drift.

II. BIO-INSPIRED ANOMALY DETECTOR

The neurons are the fundamental component for information processing in SNNs and are connected through

synapses. When the membrane potential of the presynaptic neuron is greater than a threshold value, it fires and a spike is output. Research has shown that the synapse has different dynamic effects on the neuron, such as the excitatory and inhibitory [2]. In this paper, we use the dynamic synapse model which is a phenomenological model of neocortical synapses [2]. The amount of generated postsynaptic current depends on the synaptic probability of release (PR) rate, as the approaches of [3], [4] demonstrated that the synaptic neurotransmitter is released based on a failure and success mechanism, i.e. it is transmitted based on a probability. For the neuron model, the leaky integrate and fire neuron (LIF) model [5] is used in this approach.

Fig. 1 shows the anomaly detection method for the sensor data. It includes a data encoding component, one excitatory synapse (ES), one inhibitory synapse (IS), and one spiking neuron. The ES and IS are associated with different PRs where the PR of ES (PR_E) is always high, and the PR of IS (PR_I) depends on the input data states. Based on the circuit in Fig. 1 and different PR_I assignments, the anomaly detection method is proposed. A rate-based encoding scheme is used where the sensor data (S_d) is mapped to the frequency of spiking train (f) using *Mapping*: $f \leftarrow S_d$. When the presynaptic spike train is presented to the synapses and its frequency variation is small, PR_I is set high. The spike train initiates the ES and IS to produce an excitatory and inhibitory responses, respectively. When the sum of the two synapses is below the neuron firing threshold (v_{th}) the neuron does not fire, i.e. no anomaly is detected. However, this is not the case when the frequency of input spike train has a rapid change. In this scenario, PR_I is set to low (zero) which prevents the IS producing the inhibitory response. Then, under the stimulus of ES, the neuron membrane potential crosses the v_{th} , and the neuron fires indicating an anomaly is detected. The anomalies for the sensor data is divided into positive and negative anomalies in this approach. When the sensor data has a rapid increment beyond the normal range, it is defined as a positive anomaly. Similarly, if the sensor data has a rapid decrement beyond the normal range, a negative anomaly occurs. For the positive anomaly, the PR_I is calculated based on

$$PR_I(t) = \begin{cases} 1, & \frac{ISI(t)}{ISI(t-1)} \geq Th_c \\ 0, & \frac{ISI(t)}{ISI(t-1)} < Th_c \end{cases} \quad (1)$$

where the ISI is the value of inter-spike interval, Th_c is the ISI changing threshold which is a constant value. For the negative anomaly detection, the PR_I can be calculated similarly after changing the comparison with Th_c .

The hardware architecture of the proposed method is shown in Fig. 2. The encoding component converts the sensor data to the spike train, and the PR_I calculation component outputs the real-time PR_I values according to equation (1). The IS and ES inject the current into the neuron, which outputs spikes if an anomaly is detected. One of the key applications of this research is to apply the proposed method to mobile robotics which work in critical task applications. The modular blocks allow the tuning of the IS and ES synapses for different gas sensors. This hardware detection mechanism permits the integration to a full hardware SNNs in areas such as robotics [6], [7] where the classification of the gas anomaly can be performed.

III. RESULTS

Simulation results of ES, IS and neurons. In this experiment, the input spike train is fixed, but PR_I is set to be both low and high to observe the behaviours of the synapses and spiking neurons. Fig. 3 shows the ES and IS responses, and neuron membrane potential when $PR_I = 1$. It can be seen that under the stimuli of input spikes, the ES and IS produces the positive and negative responses, respectively, which negate each other when summed at the neuron side. Therefore, the membrane potential is very low (zero) and below the threshold for firing, v_{th} , and as a result the neuron does not fire. However, if the $PR_I = 0$, the IS does not have the negative response due to the low PR. The neuron receives the positive current from ES leading to the build-up of the postsynaptic potential. The results in Fig. 4 show that when the membrane potential is greater than the v_{th} , the neuron fires and outputs the spikes which indicate that an anomaly has been detected.

Anomaly detection of chemical gases. The proposed method is applied to the anomaly detection for chemical gas sensors where a gas sensor board is used containing six low-cost gas sensors and a combined temperature/humidity sensor. The outputs of the gas sensors are all connected via a low-pass filter to a 12-bit ADC device which connects to I2C bus of a microcontroller. Each gas sensor is sensitive to specific substance(s). The chemical substances used in the experiment are surgical spirit and isobutanol. The substances are exposed to the gas sensors for a time period and then were moved away. This procedure was repeated over 10 times for each chemical substance. The data was collected between across periods of 400-600 seconds by the embedded hardware system and was transmitted to the computer for data analysis. When the chemical substances are presented to the sensors, the output values of the sensors increases from its baseline value. Thus they are positive anomaly detections for these experiments.

Fig. 5(a) shows the experimental results for the chemical substance of surgical spirit. The time points when the surgical spirit is close to the gas sensor were recorded manually which are shown by the top vertical red. It can be seen that when the surgical spirit is present, the sensor output data has a rapid change, as shown by the peaks. This rapid change makes the PR_I low and the neuron output spikes which indicate anomalies are detected. The time at which the anomaly was detection by the bio-inspired detector is marked by the top vertical blue squares. Fig. 5(a) demonstrates that the proposed method can detect the anomalies successfully. The advantage of the proposed method lies in its detection capability when the sensor experiences drift. This is analysed in the experiments of Fig.

5(b) and (c). In order to evaluate the detection performance under the conditions of sensor drifts, a synthetic dataset was created based on the original dataset and a sensor drift parameter. For example, if the drift parameter is 50%, i.e. then the sensor data has an increment of zero to 50% proportionally from the first to the last sample. Fig. 5(b) shows the sensor data with a fixed 50% drift, and its anomaly detection results. It can be seen that even when the sensor has a drift, the proposed method can successfully detect the anomalies. The proposed method is also evaluated by a various drift parameter. In Fig. 5(c), the sensor value increases based on a 50% drift, then decreases based on 50% drift, as shown by dashed brown in Fig. 5(c). The top blue with square markers show that the proposed method is able to detect the anomalies under the varied drifts. Fig. 5(a-c) demonstrate the proposed method can detect the anomalies under different conditions, such as the normal, fixed and varied drift conditions. This capability is due to the proposed method using the rate of change in (1) for the detection, which minimises the effects of sensor drift. The proposed method is further evaluated for another chemical substance of isobutanol. Fig. 5(d-e) show the experimental results for regular data, and again with fixed and varied drifts. It can be seen that the anomalies of isobutanol are detected correctly under all three different conditions. In summary, Fig. 5 demonstrates the anomaly detection capabilities of the proposed method, which can be used for the platforms/devices using the hardware chemical gas sensors.

Hardware resource utilizations. The proposed anomaly detector method was implemented on the Xilinx Virtex-7 XC7VX485TFFG1761-2 FPGA device. It uses 30 DSP48Es, 3,504 Flip Flops and 5,035 LUTs. As the DSP48E is a limited resource for the FPGA devices, the usage of different components of the proposed method is also analysed. The synapse and neuron components use 22 and 5 DSP48Es, respectively. As the top design includes some mathematical operations, it also uses 3 DSP48Es. It can be seen that the synapse component occupied the largest DSP48Es than others due to its complex model. However, this can be minimised using the CMOS implementations [1] or approximations [8], e.g. the authors have prototyped a highly optimised CMOS-based hardware dynamic synapse, shown to consume only $2.4 \times 10^{-7} mm^2$ in area [1]. This demonstrates the advantages of low cost hardware implementations over conventional approaches (e.g. [9]). Therefore, the proposed anomaly detector method make it possible to be used in embedded hardware systems (which is one main aim of this research and future work), such as the robotic mobile car [10].

IV. CONCLUSION

In this paper, a novel bio-inspired anomaly detection method was proposed. It uses the excitatory/inhibitory synapses and spiking neuron to detect the anomalies for the chemical gas sensor data. Experimental results showed that the proposed method can minimise the false-positive detections due to the sensor drift problems. The hardware implementation results demonstrate the potential for efficient use in embedded systems such as robots with a range of possible applications (e.g. security, hazardous scene assessment).

REFERENCES

- [1] Y. Chen, L. McDaid, S. Hall, and P. Kelly, "A Programmable Facilitating Synapse Device," in *IEEE International Joint Conference on Neural Networks (IJCNN)*, 2008, pp. 1615–1620.
- [2] M. Tsodyks, K. Pawelzik, and H. Markram, "Neural Networks with Dynamic Synapses," *Neural Comput.*, vol. 10, no. 4, pp. 821–835, May 1998.
- [3] J. Wade, L. McDaid, J. Harkin, V. Crunelli, and S. Kelso, "Self-repair in a bidirectionally coupled astrocyte-neuron (AN) system based on retrograde signaling," *Front. Comput. Neurosci.*, vol. 6, no. 76, pp. 1–12, 2012.
- [4] M. Navarrete and A. Araque, "Endocannabinoids potentiate synaptic transmission through stimulation of astrocytes," *Neuron*, vol. 68, no. 1, pp. 113–126, 2010.
- [5] W. Gerstner and W. M. Kistler, *Spiking neuron models: Single neurons, populations, plasticity*. Cambridge University Press, 2002.
- [6] J. Liu, J. Harkin, L. P. Maguire, L. J. McDaid, and J. J. Wade, "SPANNER: A self-repairing spiking neural network hardware architecture," *IEEE Trans. Neural Networks Learn. Syst.*, pp. 1–14, 2018 (In press).
- [7] A. P. Johnson, J. Liu, A. G. Millard, S. Karim, A. M. Tyrrell, J. Harkin, J. Timmis, L. J. McDaid, and D. M. Halliday, "Homeostatic fault tolerance in spiking neural networks A dynamic hardware perspective," *IEEE Trans. Circuits Syst.*, vol. 65, no. 2, pp. 687–699, 2018.
- [8] A. P. Johnson, D. M. Halliday, A. G. Millard, A. M. Tyrrell, J. Timmis, J. Liu, J. Harkin, L. McDaid, and S. Karim, "An FPGA-based hardware-efficient fault-tolerant astrocyte-neuron network," in *IEEE Symposium Series on Computational Intelligence*, 2016, pp. 1–8.
- [9] J. A. Hilder, N. D. L. Owens, P. J. Hickey, S. N. Cairns, D. P. A. Kilgour, J. Timmis, and A. Tyrrell, "Parameter optimisation in the receptor density algorithm," in *International Conference on Artificial Immune Systems*, 2011, pp. 226–239.
- [10] J. Liu, J. Harkin, L. McDaid, D. M. Halliday, A. M. Tyrrell, and J. Timmis, "Self-repairing mobile robotic car using astrocyte-neuron networks," in *International Joint Conference on Neural Networks*, 2016, pp. 1379–1386.

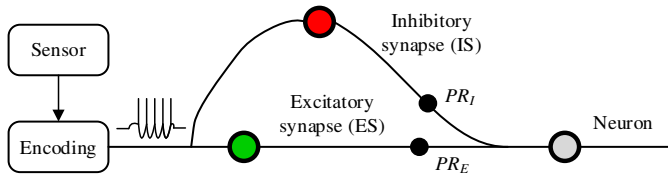


Fig. 1. Bio-inspired anomaly detector including an encoding component, one ES and IS, and one neuron. The ES and IS are associated with PR_E and PR_I , respectively.

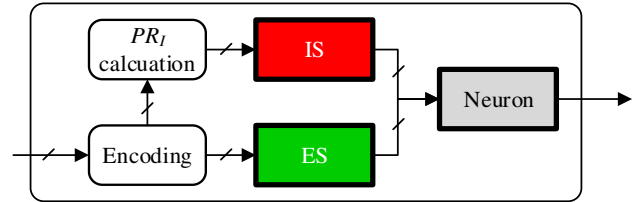


Fig. 2. Hardware architecture of the proposed method.

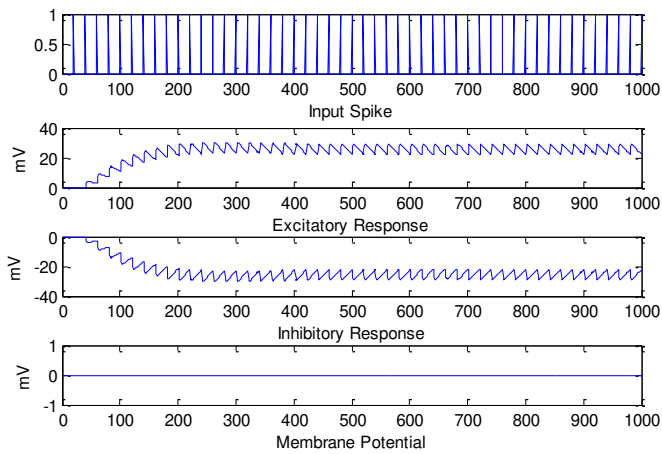


Fig. 3. Simulation results when $PR_I = 1$. If this case, the ES and IS produce the positive and negative responses, respectively, which negate each other when summed at the neuron side and thus the membrane potential of the neuron is very low (zero).

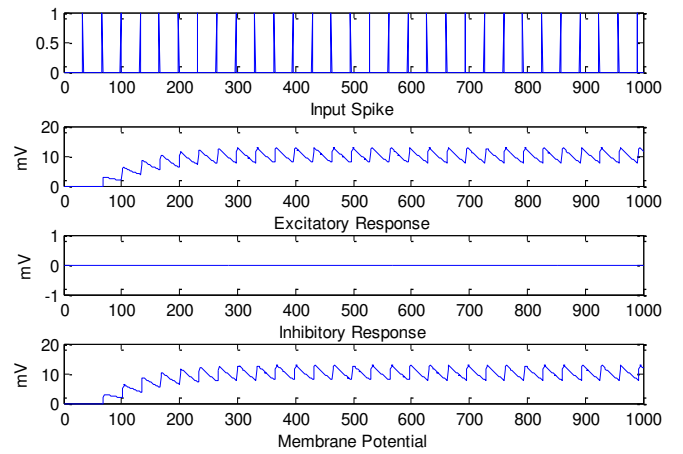


Fig. 4. Simulation results when $PR_I = 0$. In this case, the ES produces the positive responses and the IS does not have a negative response due to low PR_I . This enables the builds up of the membrane potential. When it is greater than the threshold, the neuron fires.

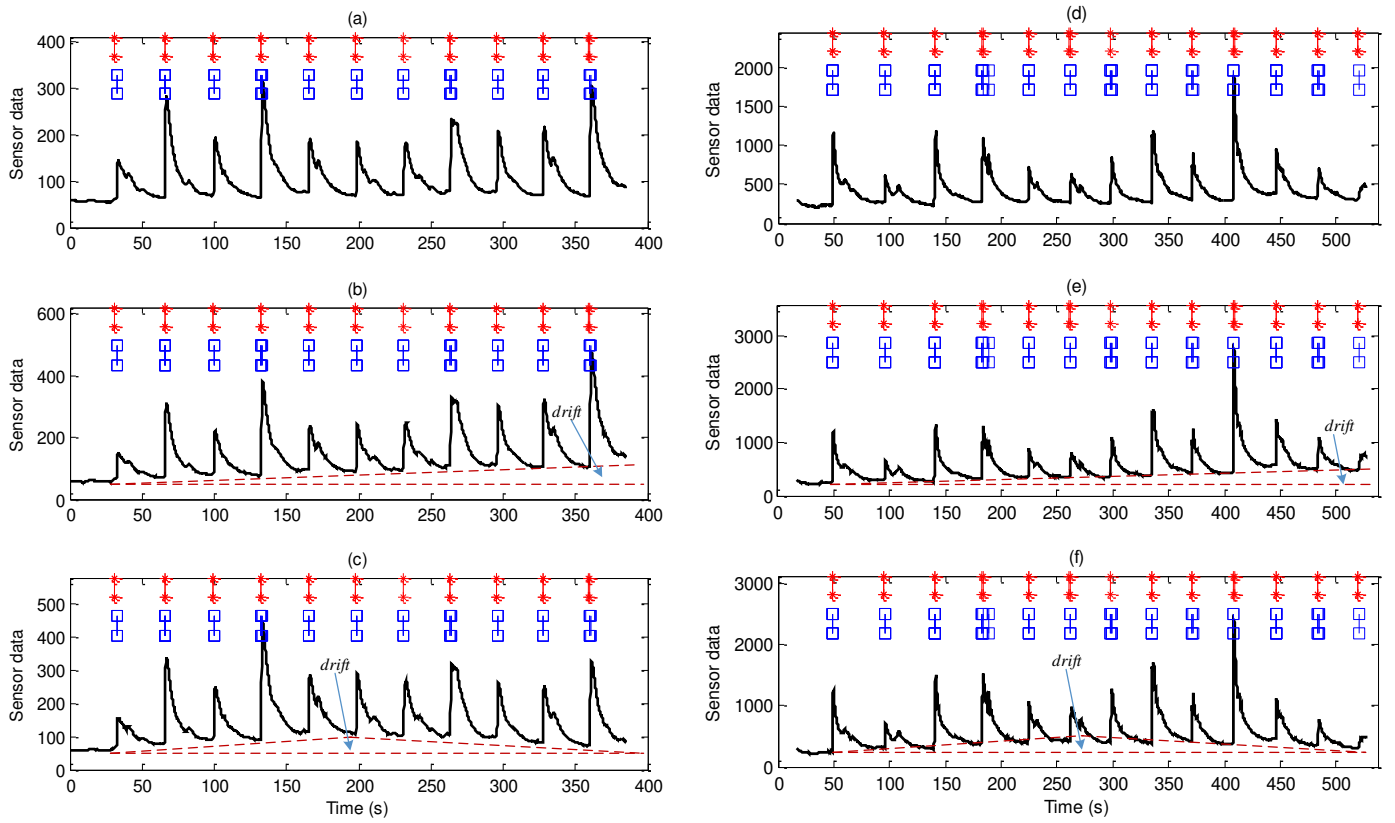


Fig. 5. Anomaly detection results for the surgical spirit (shown by (a-c)) and isobutanol (shown by (d-f)). (a, d). Regular sensor data without drift. (b, e). Fixed drift of 50%. (c, f). Varied drifts. The black bottom represents the sensor data. The top vertical red with star marker represents the manually recorded time point when the gas is presented to gas sensor. The top vertical blue with square marker represents the time point when the anomaly is detected using the proposed method.